Intermolecular Twist Defects in Extended-Chain Polymers

David C. Martin

Materials Science and Engineering, 2022 H. H. Dow Building, The University of Michigan, Ann Arbor, Michigan 48109-2136

Received April 6, 1992

ABSTRACT: Here the geometry and general properties of intermolecular twist defects in extended-chain polymer fibers are introduced. These defects are conceived as a total twisting of two or more polymer molecules about one another in the solid state. The structure and impact on mechanical properties of intermolecular twist defects in extended-chain polymer solids were explored using molecular mechanics simulations (PolyGraf and CERIUS software packages on a Silicon Graphics 4D25G workstation). The intermolecular twist defects were topologically entrapped in the molecular simulation by first creating a two-chain unit cell under triply-periodic boundary conditions and then connecting the tail of chain 1 to the head of chain 2 and vice versa. The distance between defects (the reciprocal of which is the defect density) was systematically varied by increasing the length of the simulation in the chain direction. The characteristics of these intermolecular twist defects were then examined for a particularly important extended-chain polymer system: poly(*p*-phenylenebenzobisoxazole) (PBZO). The simulation results indicate that for PBZO the internal energy of these defects is approximately 100 kcal/mol, primarily due to an increase in the energy of bond torsions. An estimate of the change in the modulus of PBZO fibers as a function of the twist defect density is also obtained. Introducing one defect at every lattice site causes a reduction in the theoretical modulus by a factor of approximately 2. Other salient features of these defects such as the distinction between left and right handedness, mechanisms for motion, and the influence on the slip behavior are also discussed. Finally, these results are compared to a constitutive relationship derived from the elastic analysis of twisted wire rope.

Introduction

Certain polymer material systems have a microstructure in which the chains exist in the solid state in a fully extended conformation. These include the aromatic polyamides such as poly(*p*-phenyleneterepthalamide) (PPTA), the rigid-rod polymers poly(*p*-phenylenebenzobisthiazole) (PBZT) and poly(*p*-phenylenebenzobisoxazole) (PBZO), gel-spun polyethylene (PE), and solid-state polymerized poly(diacetylenes). Fibers prepared from extended-chain polymers typically have high strength ($\sigma_t \approx$ 4 GPa) and stiffness ($E_t \approx$ 400 GPa), and have therefore found widespread interest for light-weight, high-performance structural applications.

The structure and properties of extended-chain polymers have been the subject of intense interest.[1] Here, we focus our attention on PBZO (Figure 1), which was developed at Wright Patterson Air Force Base (Dayton, OH) and is now being explored for possible commercialization by Dow Chemical Co. (Midland, MI). Studies of the PBZO microstructure by high-resolution electron microscopy (HREM) have revealed the evolution of the local molecular structure of PBZO as a function of the processing condition.[2] While the microstructural details of extended-chain polymers are now better understood, there is still a need to use this information to develop better constitutive models for characterizing macroscopic materials properties. This would make it possible to optimize properties by altering processing conditions. It would also aid in the design and synthesis of new polymer molecules for improved mechanical performance.

Theoretical studies of isolated, extended polymer chains have now been accomplished in some detail. Initially, information such as the theoretical tensile modulus and details about molecular-scale deformation were obtained.[3] More recently it has been possible to model the entire stress–strain response.[4] Although the analysis of individual molecules is an important first step in understanding the behavior of polymer solids, there are legimate concerns about how to relate these studies to systems in the condensed state. In particular, there is now a need to identify and isolate structural defects in order to assess their impact on macroscopic properties.

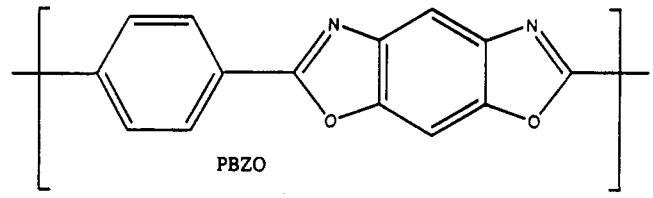

Figure 1. Chemical structure of *cis*-PBZO.

Several single-chain defects in polymer crystals have been described by Reneker and Mazur.[5] Molecular mechanics simulations of chain defects in extended-chain polyethylene led van der Werff et al.[6] to conclude that the critical defects were taut tie molecules and entanglements in amorphous domains. Noid et al. simulated the dynamics of internal chain twists in polyethylene crystals, but did not allow the chains to twist with each other.[7]

Here, we introduce and analyze multiple-chain defects we define as "intermolecular twist defects". These defects are conceived as a local twisting of at least two chains about one another (Figure 2). These twists represent local "physical entanglements" between the chains. Experimental evidence consistent with local chain twisting has been found in HREM images of axial chain invariant (ACI) grain boundaries[8] in the extended-chain polymers PBZT[9] and PBZO.[2] These lattice images showed fringes characteristic of side-to-side packing (0.55 nm in PBZO) meeting fringes with the face-to-face spacing (0.35 nm in PBZO) in the direction of the chain axis. These results are consistent with a structural model in which the chains locally twist as they traverse the grain boundary. This model is similar to the twist grain boundary proposed for polyethylene by Mazur and Reneker.[5]

The intent of this paper is to introduce the geometry of intermolecular twist defects, describe the procedures used to analyze the salient features of the defects, and then discuss the implications of these calculations. In particular, physical situations in which these sorts of defects could play an important or predominant role in

0024-9297/92/2225-5171$03.00/0

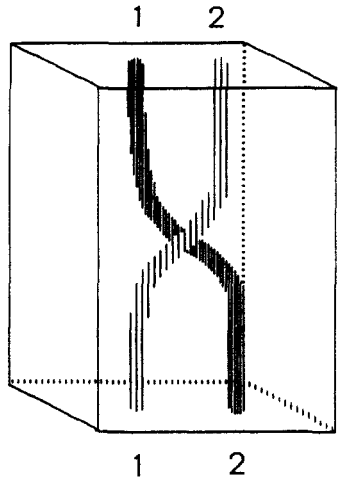

Figure 2. Schematic diagram of an intermolecular twist defect. The defects are created in the simulation by creating a two-chain unit cell and then breaking the chains. The chains are reconnected by joining the head of chain 1 to the tail of chain 2 and vice versa.

determining macroscopic properties of extended-chain polymer fibers are described. We show how to calculate the energy required to form a twist defect (for PBZO, approximately 100 kcal/mol), and demonstrate how to determine the effect of the twist defect density on macroscopic properties such as the theoretical tensile modulus. For PBZO, having one twist defect at every lattice site causes a reduction in the tensile modulus by a factor of approximately 2. Future studies will be necessary to fully determine the validity and applicability of these theoretical assertions, and to address how the behavior of these twist defects changes from one polymer material system to another.

Procedure

The simulations presented in this work were generated using the PolyGraf and CERIUS software packages which are both commercially available from Molecular Simulations Inc. These software packages have been used with reasonable success to simulate the structure and properties of extended-chain polymers.[10] A significant advantage that both of these simulation packages possess is the ability to analyze the energy of the molecules under triply-periodic boundary conditions. This analysis is realized through an Ewald sum approach where the energy of the crystal is calculated in Fourier space by summing over each reciprocal lattice site.[11] In triply-periodic boundary conditions it is possible to envision the simulation as an infinite array of cells each containing an identical copy of any given cell. This means that if a twist defect were to move across the simulation boundary, an identical copy of it would reappear on the other side.

Simulations in PolyGraf used the Dreiding II force field parameters.[12] The Fletcher–Powell minimization scheme with a gradient convergence criterion of 0.1 kcal/mol seemed to give a faster, more reproducible minimum than the default conjugate gradient technique. Convergence of the model was usually achieved in approximately 500 steps, which could amount to 12 h of computer time or more on a Silicon Graphics 4D25G workstation. In these calculations we followed the default procedure of ignoring electrostatic interactions due to concerns about the reliability of current algorithms for calculating charge equilibration.[12]

PBZO Crystal Structure

Before proceeding with an analysis of defects in PBZO, it was first necessary to resolve some outstanding questions about the structure of crystalline PBZO itself. By wide-angle X-ray scattering (WAXS), Fratini and Adams have determined the structure of PBZO to be monoclinic, with unit cell parameters of a = 1.120 mm, b = 0.3540 nm, c = 1.2050 nm, α = 90°, β = 90° and γ = 101.3°.[13] The microstructure of PBZO as a function of processing was studied by WAXS, selected area electron diffraction (SAED), bright- and dark-field transmission electron microscopy (BF and DF TEM), and high-resolution electron microscopy (HREM) by Martin and Thomas.[2] These researchers demonstrated that it was necessary to consider a random $\pm {}^1/_4c$ shift of laterally associated PBZO chains to obtain a structural model consistent with the available experimental data.

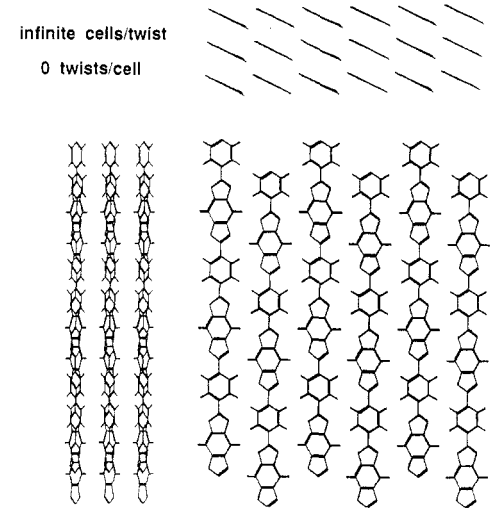

Figure 3. Minimum energy conformation of PBZO obtained using a two-chain unit cell.

To construct the PBZO crystal two monomer units of PBZO (Figure 1) were created using the "draw" facility in PolyGraf. These two units were terminated with hydrogen atoms, minimized in energy, oriented parallel to one another, and then placed in a periodic unit cell. Both monomers were "polymerized" by extending the system, removing the terminal hydrogen atoms, and connecting the head of each monomer unit to the image of its own tail in the neighboring unit cell. The polymer molecules so obtained were allowed to minimize their energy within this unit cell. At the start of the simulation there was no axial shift between the PBZO molecules. All the internal coordinates of the atoms as well as the unit cell parameters were allowed to be variable.

Figure 3 shows the minimum energy configuration of crystalline PBZO achieved by this approach. As predicted by experiments,[2] the molecules adopt a local packing in which laterally associated neighboring molecules are displaced by + or $-{}^1/_4c$ with respect to one another. From the view down the chain axis it is evident that the benzene ring and heterocyclic group are nearly coplanar, a result consistent with studies of isolated chains.[3] The unit cell parameters at the apparent minimum (a = 1.0696 nm, b = 0.3684 nm, c = 1.2158 nm, α = 90.001°, β = 90.672°, γ = 85.677°) are in reasonable but not exact agreement with the experimental results of Fratini and Adams.[13] The angle between the direction normal to the PBZO benzene ring (and heterocyclic group) and the a axis is approximately 64°. Figure 4 is a magnified view of the minimum energy configuration of the PBZO crystal viewed along the [010] direction. The benzene ring on a given PBZO chain fits into a space between the benzene ring and heterocyclic group on a neighboring chain.

Figure 5 shows the energy of the PBZO crystal as a function of the axial shift of the second PBZO molecule, calculated using the CERIUS software package. There are predominant minima at relative positions of approximately $\pm {}^1/_4c$ between molecules. The maximum energy (150 kcal/mol above the minimum) occurs when the PBZO

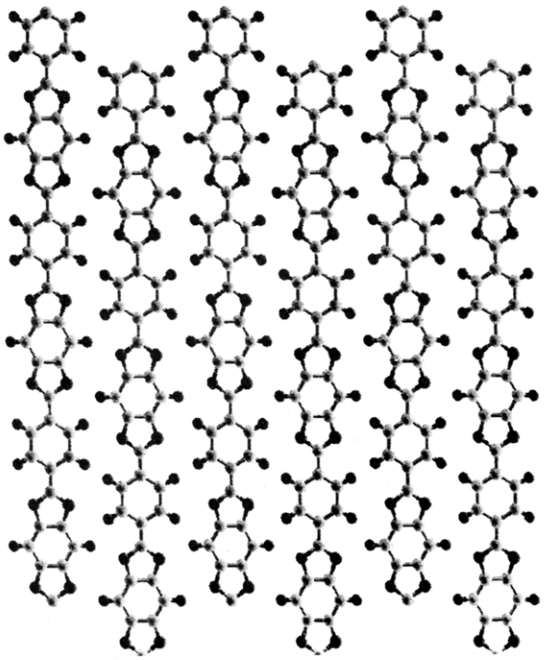

Figure 4. Close-up of minimum energy conformation. Lateral chains are displaced $\pm^1/_4c$ with respect to one another.

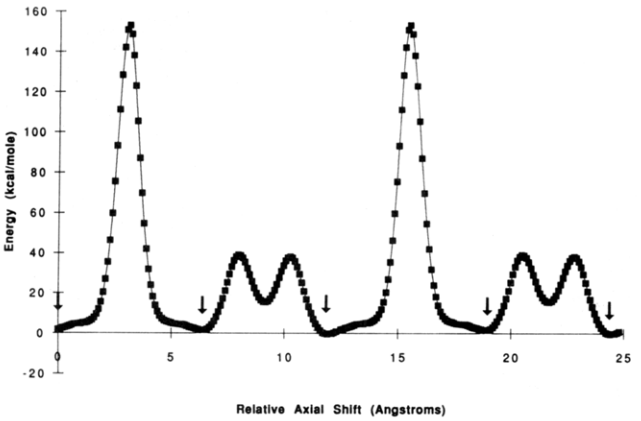

Figure 5. Energy of the PBZO crystal as a function of axial shift in the c direction. Minima at positions of approximately $\pm^1/_4c$ are indicated.

molecules are both placed at the same position (i.e., with all the benzene rings and heterocycles arranged in planes strictly perpendicular to the chain axis). This energy barrier is significantly higher than that estimated from early studies of PBZO interactions (3 kcal/mol).[14] However, these initial approaches only considered single-neighbor interactions between chains, not a triply-periodic unit cell.

The tensile modulus of PBZO was calculated by applying a stress in the chain direction and allowing the molecules to reequilibrate. By measuring the increase in the unit cell size caused by this deformation, we obtained a value of 511 GPa for the theoretical tensile modulus of perfectly crystalline PBZO. This value compares reasonably well with previous theoretical results by Tashiro and Kobayashi (460 GPa).[15,16] Weirshke[3] and Adams et al.[4] obtained a value of 730 GPa using AM1 calculations on isolated molecules.

Intermolecular Twist Defects

A schematic diagram of an intermolecular twist defect is shown in Figure 2. To introduce the defects, a two-chain unit cell was constructing using the energy-minimized structure for the perfect crystal. The two chains

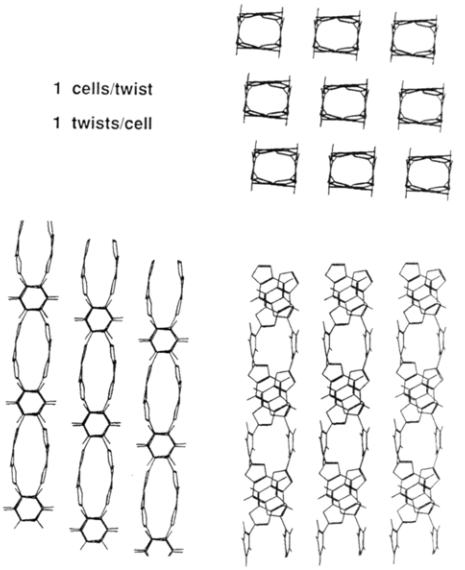

Figure 6. Minimized configuration with one unit cell and one twist, corresponding to a twist density of one twist per unit cell. Most of the distortion of the molecule takes place in the single bond.

were both cleaved at the single bond between the benzene ring and the heterocyclic group. The end of chain 1 was then attached to the head of chain 2 and vice versa. As discussed, this procedure introduces a topologically trapped twist that cannot escape because of the three-dimensional nature of the periodic boundary conditions. Both left- and right-handed examples of these twist defects are possible, although because of the symmetry of the PBZO molecule these do not differ significantly in this instance. However, with molecules that adopt helices with specific handedness this will become an important distinction. Also, it will be necessary to consider handedness in the analysis of defect–defect interactions.

The ability to change the length of the simulation in the chain direction makes it possible to systematically alter the effective density of the twist defects. As the length of the simulation increases, the twist defect density decreases. Since there is one twist defect in the simulation, the reciprocal of the simulation length (defects per unit cell) is the defect density.

Figures 6 and 7 illustrate the structural changes introduced as a function of twist defect density. Figure 6 shows the minimized configuration with one twist defect per unit cell. The primary area of torsional deformation is the carbon–carbon single bond connecting the benzene ring to the heterocyclic group. Figure 7 shows the geometry of the twisted PBZO molecules after energy minimization at a twist defect density of 0.25 per unit cell. As the defect density decreases, the defects begin to adopt a configuration in which they are arranged in planes whose normals make a significant angle to the primary orientation axis. This is evidently because the twist defects introduce a local expansion of the crystal lattice and therefore have an unfavorable energy of interaction with one another.

It is possible to analyze the changes introduced into the PBZO molecules during twisting in detail. Figures 8–10 illustrate the variation of several important geometric parameters as a function of twist defect density. As the molecules become more twisted there is a systematic decrease in the length of the c-axis repeat distance (Figure 8). It is also possible to measure the local misorientation of the chain axis with respect to the primary axis of orientation (Figure 9). As expected, the misorientation systematically increases with twist defect density. The twisted simulations have a theoretical density on the order

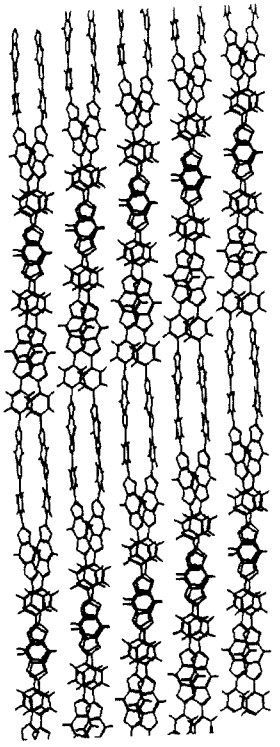

Figure 7. Minimized configuration with four unit cells and one twist, corresponding to a twist density of $^1/_4$ twist per unit cell. As the defects move farther apart, they begin to line up into planes which are no longer perpendicular to the axis of orientation. This is apparently due to the fact that there is an unfavorable interaction between the twist defects.

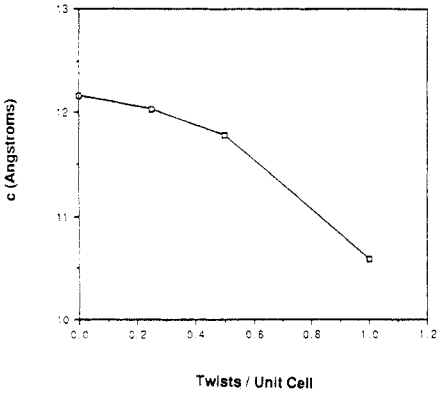

Figure 8. Length of the c-axis repeat distance as a function of twist defect density. As the amount of twisting increases, the c-axis repeat distance decreases.

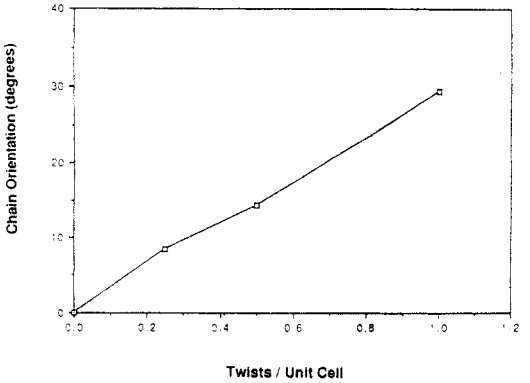

Figure 9. Local misorientation of the PBZO chain as a function of defect density. As the amount of twisting increases, the misorientation increases.

of 1.45 g/cm^3 as compared to 1.63 g/cm^3 for the perfect PBZO crystal (Figure 10). This density decrease occurs even for small twist defect densities. At the highest defect

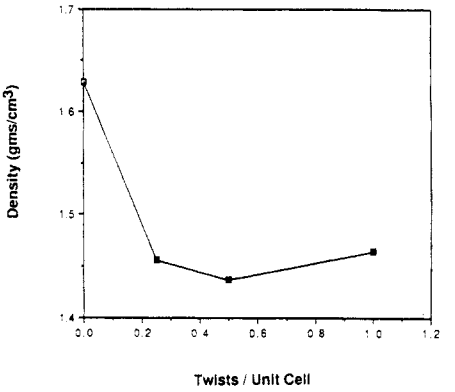

Figure 10. Theoretical density as a function of twist defect density. The density drops from a value of 1.63 for the perfect PBZO crystal to a range of about 1.45 for the twist defects. At the highest degree of twisting the density begins to increase again; the effect is probably due to the formation of local favorable packing contacts (Figure 6).

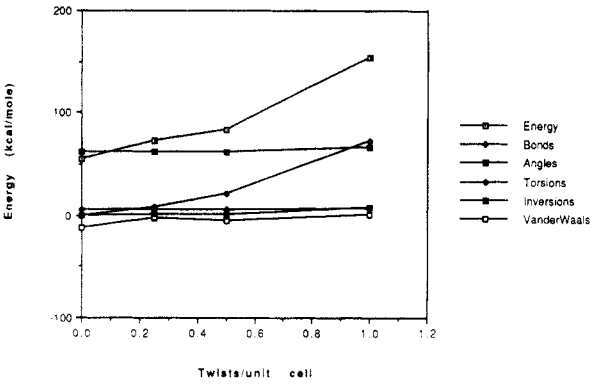

Figure 11. Relative energies of bond stretching, bond angle bending, bond inversions, bond torsions, and nonbonded interactions as a function of defect density. The primary contribution to the twist defect energy arises from the energy of bond torsions. The energetic penalty for introducing a twist defect at every lattice site in PBZO is 100 kcal/mol.

density the theoretical density begins to increase, perhaps due to local accomodations in chain packing from the shape of the PBZO molecule.

Figure 11 illustrates the change in the energy of the twisted simulations as a function of the defect density. The primary source of the increase in energy during twisting comes from the energy of bond angle torsions. For PBZO, the increase in energy required to introduce one twist defect at every unit cell position is approximately 100 kcal/mol.

A central issue was to determine the influence of these twist defects on mechanical properties. To accomplish this, we examined the molecules under an applied stress in the chain direction. Figure 12 shows the change in the energetics of untwisted PBZO molecules as a function of tensile stress. The primary contribution to the tensile response arises from an increase in the energies of bond angle stretching and bending. In compression the increase in energy is due to nonbonded van der Waals interactions. For comparison Figure 13 shows the energetic response as a function of stress for the simulation with one twist defect per lattice site. As before, the response in tension arises primarily from the energies of bond angle stretching and bending. However, the compressive response now has a significant contribution not just from van der Waals forces but also from an increase in the energy of bond torsions.

It is worth emphasizing that neither of these fully dense simulations (perfect PBZO crystals or perfect twisted PBZO crystals) show a compressive instability at ~0.4 GPa as seen in simulations of isolated chains and in

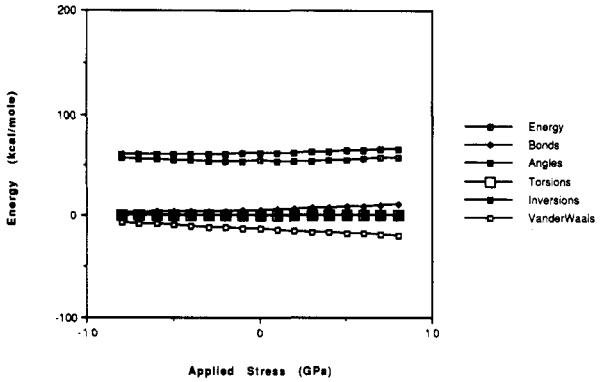

Figure 12. Relative energies of the untwisted PBZO molecule as a function of applied stress. In tension, the energetic contribution comes from bond stretching and bond angle bending. In compression, the energy of nonbonded van der Waals contacts increases.

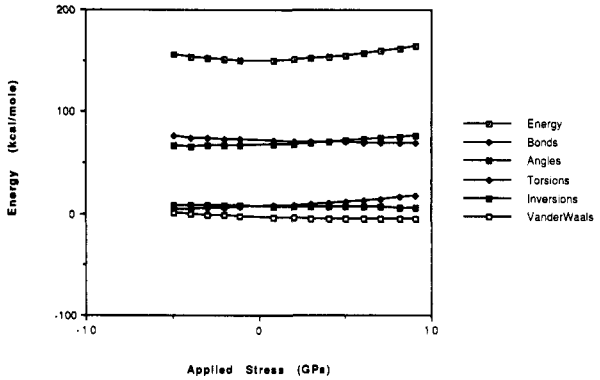

Figure 13. Relative energies of the twisted PBZO molecule (1 twist/cell) as a function of applied stress. As before, the energetic contribution in tension comes from bond angle stretching and bond angle bending. However, in compression the response is due to both nonbonded interactions as well as the energy of bond torsions.

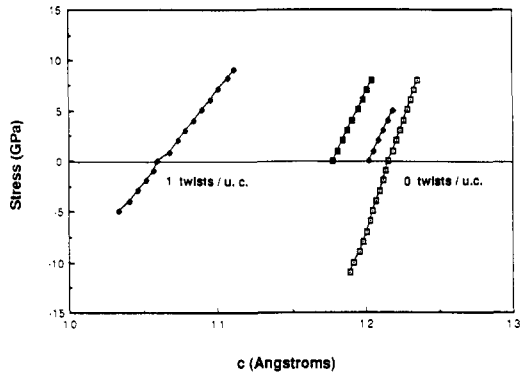

Figure 14. Change in c-axis repeat length as a function of applied stress and twist defect density. The slope of these lines corresponds to the theoretical tensile modulus. It can be seen that models with a higher twist defect density have a lower modulus. Also note that the models do not exhibit a compressive instability at stresses corresponding to the experimentally observed compressive failure stress (~0.4 GPa).

experiment. This suggests that local fluctuations in density are particularly important for initiating compressive failure. This is an important issue which we address in more detail in the Discussion.

Figure 14 shows the variation in the repeat distance along the chain axis as a function of applied stress and defect density. The slopes of these lines correspond to the tensile modulus. It is evident that as the chain axis repeat decreases (i.e., the twist density increases) the modulus systematically decreases. Figure 15 shows the tensile modulus as a function of twist defect density, showing this decrease in the modulus with increasing

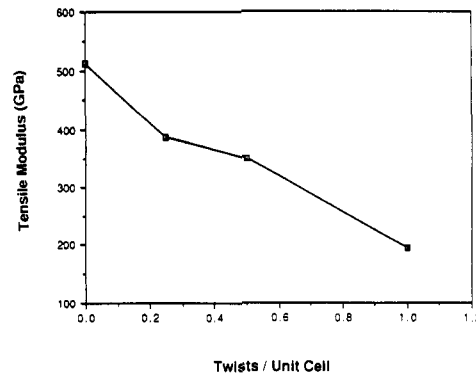

Figure 15. Change in the tensile modulus as a function of twist defect density. The theoretical modulus of the perfectly crystalline PBZO is similar in magnitude to that obtained by other studies. The twist defects cause a systematic decrease in the tensile modulus, with the tensile modulus of the sample with one twist per unit cell approximately half that of the perfect crystal.

twisting. The simulations predict that if there were one twist defect at every lattice site, the theoretical modulus of PBZO would decrease by a factor of approximately 2.

Discussion

Extended-chain polymers like PPTA and PBZO are processed from nematic lyotropic liquid crystalline solutions in a dry-jet wet spinning process. The solutions usually employ a strong acid to dissolve the polymer. The fibers are formed by quenching the solution in a bath of nonsolvent (typically water). This phase transition causes the formation of a continuous microfibrillar network[17] which is dried and heat treated under tension to optimize strength and stiffness.[18] It is reasonable to expect that intermolecular twist defects would be formed as the polymer passes through the phase transition from lyotropic liquid crystalline solution to solid polymer fiber.

The postspinning heat treatment procedure causes local areas of crystallinity to develop,[2] the dimensions of which (20 nm) are well below the average dimensions of the polymer molecules themselves (100 nm). This means that, as the lateral order between molecules increases during annealing, it is likely that intermolecular twist defects could be trapped into regions between two crystallites. Since the defects cause a local variation in density, regular modes of defect segregation into grain boundaries could result in crystallites with well-defined shapes, and therefore these materials would exhibit characteristic and unique small-angle X-ray scattering (SAXS) patterns. This proposed segregation of twist defects forms the basis of axial chain invariant (ACI) grain boundaries, using the nomenclature suggested by Martin and Thomas.[8] Experimental evidence for ACI boundaries has been obtained in HREM images of PBZT[9] and PBZO.[2,8] Similar suggestions about twist defect segregation to grain boundaries have been presented by Reneker and Mazur.[5]

With this mechanism of twist defect generation in mind, it is reasonable to expect to see twist defects in extended-chain polymers processed from solution or from the gel state (i.e., in PPTA, PBZT, PBZO, and PE). Our research group is currently involved in studies of solid-state polymerizable diacetylenes in order to isolate the impact of specific defects on local structural variations and macroscopic properties. Our goal is to systematically introduce grain boundary defects into ordered polymer systems in a well-controlled and reproducible manner.

In practice, intermolecular twist defects would not strictly involve two unique chains twisting about one another, but instead would be randomly distributed from chain to chain. In this manner, one chain may be twisted

with several of its neighbors. Prasad and Grubb examined the (002) reflection in extended-chain polyethylene by synchrotron X-ray scattering and found that the peak shifts to a lower angle and broadens under tension.[19] They interpreted these results in terms of a distribution in the "stressed state". In other words, certain chains are more "twisted" than others.

A critical comparison of the results of these simulations with experiment reveals that twist defects alone do not provide a complete picture of the polymer solid state. In extended-chain polymer fibers the density is reasonably close to that of the perfect crystal, and the amount of misorientation is small.[1,2] If we assume that the density of the fiber is 1.5 g/cm^3 and the amount of misorientation 2.0°, it is possible to estimate the effective number of twist defects by comparison with Figures 9 and 10. It is evident that the effective twist defect density in this case would be less than $^1/_{20}$ twist/unit cell. Therefore, in order to fully account for the experimentally observed variations in the modulus during postspinning processing,[16] it seems necessary to consider additional types of structural defects.

An inevitable source of defects in any polymer with finite molecular weight is chain ends. However, the concentration of chain ends should not ordinarily change as a function of processing, although their relative position may change. Martin and Thomas showed experimental evidence for an edge dislocation which was rationalized as arising from the mutual segregation of a number of chain ends oriented in the same direction.[2] Smith and Termonia examined chain ends using a kinetic model and predicted that both the strength and modulus decreased with an increasing number of chain ends, although the strength was much more sensitive to the chain end density.[20] Further simulations on the effect of chain ends are certainly warranted, and we are proceeding in this direction in our laboratory at present. We believe that a similar simulation size scaling approach should enable us to examine the transfer of stress from chain to chain through nonbonded interactions.

As we discussed earlier, these systems do not exhibit the experimentally observed compressive instability associated with kinking, although compressive instabilities are seen in isolated chain simulations.[3,4] This observation suggests that it is important to consider the influence of local density fluctuations. To address the impact of local heterogeneities in molecular packing, it should be possible to use an analysis in which the unit cell dimensions are varied in both the a and b directions. Recent results on poly(diacetylene) crystals with significant void content have shown that kinking is sensitive to the local density;[21] regions where the poly(diacetylene) crystals are below some apparently critical density do not exhibit kinking at all, while the denser poly(diacetylene) crystals kink relatively often.

It is evident that intermolecular twist defects should disrupt the uniformity of strain during shear deformation. Because of the presence of the physical entanglement of the two chains, it will no longer be possible to develop a shear strain between them. Therefore, twist defects will disrupt the uniformity of shear deformation. The heterogeneity of deformation within sheared regions inside kink bands in extended-chain polymer fibers has been observed experimentally.[22] Since twists lead to lateral interactions between chains, they should also be important in creep and long-term fatigue response.

It is possible to envision other types of defects constructed from assemblies of these and other defects. These might include chain-end dislocations, kinks, and other sorts of grain boundaries involving both tilt and twist. Reneker and Mazur have described the structure and energetic features of defects in crystalline polyethylene,[5] but it has not yet been possible to use this information to derive constitutive relationships to understand or predict material properties. To do this task properly will require significantly more atoms per simulation and a corresponding increase in the computational time required.

Figure 15 indicates that the density of twist defects in PBZO must be relatively large before there is a significant reduction in the tensile modulus. As discussed earlier, a more complete description of the microstructure of extended-chain polymers will require an analysis of additional defects, in particular chain ends and voids. Nevertheless, this result also suggests that efforts to manipulate the microstructure by material processing (i.e., changing the defect density) may only lead to a secondary effect on the ultimate mechanical properties of the polymer. It is reasonable to expect that much more significant changes in performance could occur by creativity altering the chemical structure of the molecules themselves. Current efforts in this direction include the synthesis of ladder polymers from soluble precursor polymers, and small, highly reactive cross-linkable groups which do not disrupt processing but can introduce lateral covalent bonds during a postspinning thermal treatment.[23]

Intermolecular twist defects are point defects which are apparently unique to macromolecular solids. Certain salient features which become evident after analyzing the geometry of the defects are worthy of further discussion. For example, consider first the highly anisotropic mobility of the twist defects. Because of the manner in which the two chains twist around one another, defect motion will be strictly limited to the direction of the chain axis if no covalent bonds are broken. Another topic worthy of further discussion and study is the mechanisms of defect annhilation. Annhilation is possible when a left-handed twist runs into a right-handed twist on the same two chains. Also, the twist may annhilate when it encounters a chain end. Finally, one might speculate on the possibility of twist defect sources. It is difficult to envision a means for introducing these twist defects after the molecules have been processed from the liquid crystalline mesophase. However, it might at least be feasible to design special processing routes which optimize the density of twist defects. It is not yet clear that twist defects are always to be removed or avoided, and perhaps some careful consideration about how to control them would provide a means for further optimizing the mechanical response of extended-chain polymers. For example, increasing the density of twist defects could lead to improved fiber toughness and creep resistance.

Constitutive Analysis

After considering the results of the simulations showing a decrease in the tensile modulus as a function of twisting, the similarities of twisted, stiff molecules with the elasticity of twisted wire rope were examined. The theory of wire rope has been the topic of a recent monograph by Costello.[24] Here, we demonstrate how this theory may be applied to intermolecular twist defects which are essentially two-wire ropes with no core wire. Using Costello's notation, for a wire rope constructed of an inner wire of radius R_1 surrounded by helical wires of radius R_2 twisted at a helix angle α, the amount of strain ϵ in the rope induced by an applied load is given by

$$\epsilon = \xi_1 = \xi_2 + \Delta\alpha/\tan\alpha \quad (1)$$

where ξ_1 is the strain in the inner wire, ξ_2 is the strain of an outer wire, and $\Delta\alpha$ is the change in α after loading. It is assumed that $\Delta\alpha$ is a small quantity. The rotational

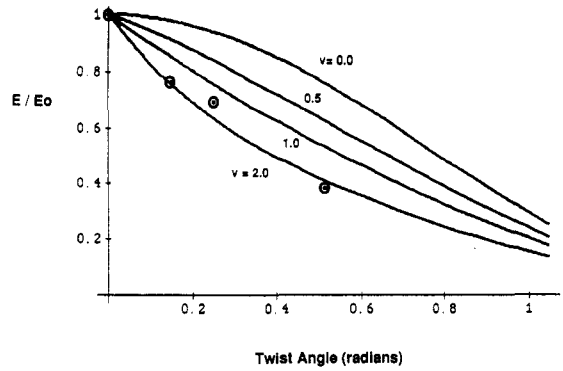

Figure 16. Comparison of the results of the simulations with the elastic analysis of wire rope made possible by the results shown in Figures 8 and 15. The only adjustable parameter in this approach is Poisson's ratio of the strand. In the figure several different choices for Poisson's ratio are shown. The best of the results of the simulation comes from a Poisson ratio equal to 2.0. Values of Poisson's ratio greater than 2.0 are peculiar, and indicate that the sample is capable of increasing its density during stress.

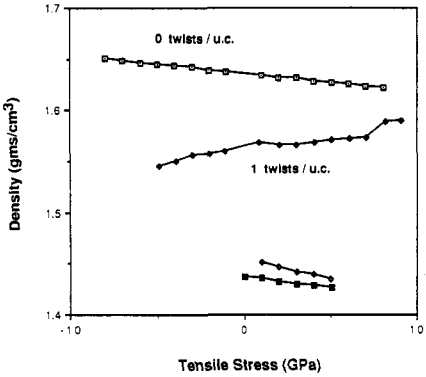

Figure 17. Density of twisted PBZO as a function of twist defect density and applied stress. The sample with the highest density of twist defects increases in density under stress, as predicted by the elastic analysis results. The phenomenon is evidently related to the increased "packing" which is promoted by additional stress when there is a sufficient amount of twisting present.

strain β_2 in an outer wire is given by

$$\beta_2 = \xi_2/\tan\alpha - \Delta\alpha + \nu(R_1\xi_1 + R_2\xi_2)/((R_1 + R_2)\tan\alpha) \quad (2)$$

where ν is the Poisson ratio of the wire strands. The modulus of a wire strand is

$$E_0 = S/\xi_2 \quad (3)$$

where S is the applied stress. Likewise, the modulus of the wire rope is

$$E = S/\epsilon \quad (4)$$

In our case, $R_1 = 0$ (there is no center wire). We also assume that since the two wires are equivalent, there is no net rotational strain (i.e., $\beta_2 = 0$). Using these boundary conditions and simplifying, we find

$$\xi_2/\epsilon = E/E_0 = 1/(1 + (1 + \nu)/\tan^2\alpha) \quad (5)$$

Here, E is the modulus of the twisted bundle, E_0 is the untwisted reference state, α is the angle of twist, and ν is the Poisson's ratio. Figure 16 shows the comparison of this equation with the twisted PBZO simulations. The best fit to the simulation results requires a value of ν equal to 2.0. This is remarkable, since values of ν greater than 0.5 require the system to increase in density under stress. However, this is precisely the situation at hand. When molecules twist about one another, pulling on the chains causes them to be forced closer together laterally. This is similar to the response of a twisted multistrand rope, or the familar woven "finger torture" device that holds on more tightly as the victim attempts to escape.

Figure 17 shows the variation in density of the simulations as a function of stress and twist defect density. At the highest twist defect density examined (1.0 twists per cell), there is indeed an increase in density under stress. Although local increases in density might occur in real fibers due to this effect, it seems unlikely that a macroscopic Poission ratio greater than 0.5 would ever be realized in practice due to the inevitable presence of heterogeneities of molecular packing over large length scales.

Acknowledgment. This work was supported in part by the University of Michigan College of Engineering and the National Science Foundation (Grant DMR-9024876). I thank P. M. Wilson and J. P. Anderson for critical review of the final draft of the paper.

References and Notes

(1) Adams, W. W., Eby, R. K., McLemore, D., Eds. *The Materials Science and Engineering of Rigid Rod Polymers*, Materials Research Society Symposia Proceedings; Materials Research Society: Pittsburgh, PA, 1989; Vol. 134.
(2) Martin, D. C.; Thomas, E. L. *Macromolecules* **1991**, *24* (9), 2450–2460.
(3) Weirshke, S. In *The Materials Science and Engineering of Rigid Rod Polymers*, Materials Research Society Symposia Proceedings; Adams, W. W., Eby, R. K., McLemore, D., Eds.; Materials Research Society: Pittsburgh, PA, 1989; Vol. 134.
(4) Adams, W. W.; Dudis, D. S.; Weirschke, S. G.; Haaland, P.D.; Shoemaker, J. R. Computational Predictions of Polymeric Single Chain Properties. *Deformation, Yield, and Fracture of Polyers, 8th International Conference*; The Plastics and Rubber Institute, Churchill College: Cambridge, U.K., 1991.
(5) Reneker, D.; Mazur, J. *Polymer* **1988**, *29*, 3.
(6) van der Werff, H.; van Duynen, P. T.; Pennings, A. J. *Macromolecules* **1990**, *23*, 2935–2940.
(7) Noid, D. W.; Sumpter, B. G.; Wunderlich, B. *Macromolecules* **1991**, *24*, 4148–4151.
(8) Martin, D. C.; Thomas, E. L. *Philos. Mag.* **1991**, *64* (4), 903–922.
(9) Boudet, A.; Martin, D. C.; Thomas, E. L. *Proceedings of the European Symposium on Polymeric Materials*, Lyon, France, 1987.
(10) Yang, X.; Hsu, S. L. *Macromolecules* **1991**, *24*, 6680–6685.
(11) Karasawa, N.; Goddard, W. A. *J. Phys. Chem.* **1989**, *93*, 7320.
(12) Mayo, S. L.; Olafson, B. D.; Goddard, W. A. *J. Phys. Chem.* **1990**, *94*, 8897–8909.
(13) Fratini, A. V.; Lenhert, P. G.; Resch, T. J.; Adams, W. W. In *The Materials Science and Engineering of Rigid Rod Polymers*, Materials Research Society Symposia Proceedings; Adams, W. W., Eby, R. K., McLemore, D., Eds.; Materials Research Society: Pittsburgh, PA, 1989; Vol. 134.
(14) Bhaumik, D.; Welsh, W. J.; Jaffe, H. H.; Mark, J. E. *Macromolecules* **1981**, *14*, 951–953.
(15) Tashiro, K.; Kobayashi, M. *Sen'i Gakkaishi* **1986**, *62*, 78–91.
(16) Tashiro, K.; Kobayashi, M. *Macromolecules* **1991**, *24*, 3706–3708.
(17) Cohen, Y.; Thomas, E. L. *Macromolecules* **1988**, *21*, 43.
(18) Allen, S. R.; Farris, R. J.; Thomas, E. L. *J. Mater. Sci.* **1985**, *20*, 2727–2734.
(19) Prasad, K.; Grubb, D. T. *J. Polym. Sci., Part B: Polym. Ed.* **1990**, *28*, 2199–2122.
(20) Smith, P.; Termonia, Y. *Polym. Commun.* **1989**, *30*, 66–68.
(21) Liao, J.; Martin, D. C. Defects in [1,6-di(n-carbazolyl)-2,4-hexadiyne] Diacetylene Crystals. *Electromagnetic and Optical Properties of the Organic Solid State*, Materials Research Society Symposia Proceedings; Materials Research Society: Pittsburgh, PA, 1992.
(22) Martin, D. C.; Thomas, E. L. *J. Mater. Sci.* **1991**, *26*, 5171–5183.
(23) Walker, K.; Markoski, L.; Moore, J.; Martin, D. *Polym. Prepr.*, manuscript in preparation.
(24) Costello, G. A. *Theory of Wire Rope*; Springer-Verlag: New York, 1990.

Registry No. PBZO, 60871-72-9.